Asymmetric q-Gaussian functions generalizing the Breit-Wigner-Fano functions

(Article begins on next page)

29 April 2024

Asymmetric q-Gaussian functions generalizing the Breit-Wigner-Fano functions

Amelia Carolina Sparavigna

Department of Applied Science and Technology, Polytechnic University of Turin, Italy

Email: amelia.sparavigna@polito.it

Torino, September18, 2023.

Abstract

Previous studies (Sparavigna, 2023) have demonstrated the Tsallis q-Gaussian functions suitable for the analysis of Raman spectra. The q-Gaussians are symmetric functions that can be used for simulating different line shapes of Raman bands. Here we propose an asymmetric form of the q-Gaussians, to generalize the Breit-Wigner-Fano profiles. Some examples are proposed, in particular a case study of the LO band of SiC.

Keywords: Tsallis q-Gaussian distribution, Breit-Wigner-Fano function, Gaussian distribution, Cauchy distribution, Lorentzian distribution, Raman spectroscopy.

---

q-Gaussian functions, also known as "Tsallis functions", are probability distributions derived from the Tsallis statistics (Tsallis, 1988, 1995, Hanel et al., 2009). The q-Gaussians are based on a generalized form of the exponential function (see discussion in Sparavigna, 2022), characterized by a continuous parameter q in the range $1 < q < 3$. As given by Umarov et al., 2008, the q-Gaussian function is based on function $f(x) = Ce_q(-\beta x^2)$, where $e_q(.)$ is the q-exponential function and C a constant. In the exponent, we use $\beta = 1/(2\sigma^2)$, with variance σ. The q-exponential has expression: $exp_q(u) = [1 + (1 - q)u]^{1/(1-q)}$, which possesses a bell-shaped profile. In the case that we have the peak of the function at position x_o, the q-Gaussian function is given as:

$$\text{q-Gaussian} = Cexp_q(-\beta(x - x_o)^2) = C[1 - (1 - q)\beta(x - x_o)^2]^{1/(1-q)}$$

For q equal to 2, the q-Gaussian is the Cauchy-Lorentzian distribution (Naudts, 2009). For q close to 1, we have the usual Gaussian form. For the q-parameter between 1 and 2, the shape of the q-Gaussian function is intermediate between the Gaussian and the Lorentzian profile. This behavior turns the q-Gaussian into a function suitable for the analysis of Raman spectra, where the spectral bands are characterized, in the same manner, by intermediate profiles between Lorentzian and Gaussian outlines (Kirillov, 2004a). Besides these two functions, which remain the most popular for fitting Raman spectra, *linear combinations* (pseudo-Voigt distributions) or *convolutions* of them (Voigt distributions) are used too (Meier, 2005). The Voigtian function is essentially a Lorentzian height weighted by a Gaussian profile.

Gaussian, Lorentzian, Voigtian and pseudo-Voigtian functions, such as the q-Gaussians are symmetric functions. In fitting the Raman bands, we have encountered peaks which are asymmetric. For instance, in the case of Diamond, (see SSRN), we had the necessity to use three q-Gaussians to fit the asymmetric Raman peak of the spectrum of synthetic diamond. Of course the presence of more bands producing what looks like an asymmetric peak can be motivated by physical reasons; in any case, an alternative approach exists to fit asymmetric profiles. The alternative is based on the use of Breit-Wigner-Fano (BWF) functions.

The BWF function is given as:

$$BWF = C \frac{\left[1 + \xi \gamma^{1/2}(x - x_o)\right]^2}{\left[1 + \gamma(x - x_o)^2\right]}$$

In it, ξ is the asymmetry parameter (see Hasdeo et al., 2014, for the use of Breit-Wigner-Fano line shapes for the Raman spectrum of graphene). We could generalize the BWF in the q-form (BFW$_q$):

q-BWF $= C\left[1 + \xi \beta^{1/2}(q-1)^{1/2}(x-x_o)\right]^2 [1 + (q-1)\beta(x-x_o)^2]^{1/(1-q)}$

However, we can further generalize the asymmetric form in the following manner:

q-BWF $= C\left[1 + \xi \beta^{1/2}(q-1)^{1/2}(x-x_o)\right]^{2\alpha} [1 + (q-1)\beta(x-x_o)^2]^{1/(1-q)}$

When q=2, α=1, we have the function BWF.

Hasdeo and coworkers are giving, in their Eq.(1), the BWF line shape composed by three terms: "a constant continuum spectrum, a discrete Lorentzian spectrum, and an interference effect between both spectra". The interference term is producing the asymmetry of the profile, according to the positive and negative values of the argument $(x-x_o)$. The dimensionless ξ parameter is "mimicking the ratio between the probability amplitude of the continuum spectra to that of the discrete spectra" (Hasdeo et al., 2014). Also in Prawer and Nemanich, 2004, we can find mentioned the asymmetry of Raman peaks according to specific effects; we find also the "phonon confinement effects for finite crystal domains" (Richter et al., 1981). In Campbell and Fauchet, 1986, we can easily see that the effects of microcrystal size on the shape of Raman spectra. In their Fig.4, an asymmetric peak for thin film of silicon on saphire (SOS) is shown.

Let us start from fitting with q-BWF the curve proposed in the Fig.3(a) by Hasdeo et al. The continuous curve is given by Hasdeo and coworkers according to a theoretical model. The curve is clearly asymmetric. The fitting result is shown in the following Figure. We can see that the q-BWF is a BWF function, as expected by the theory.
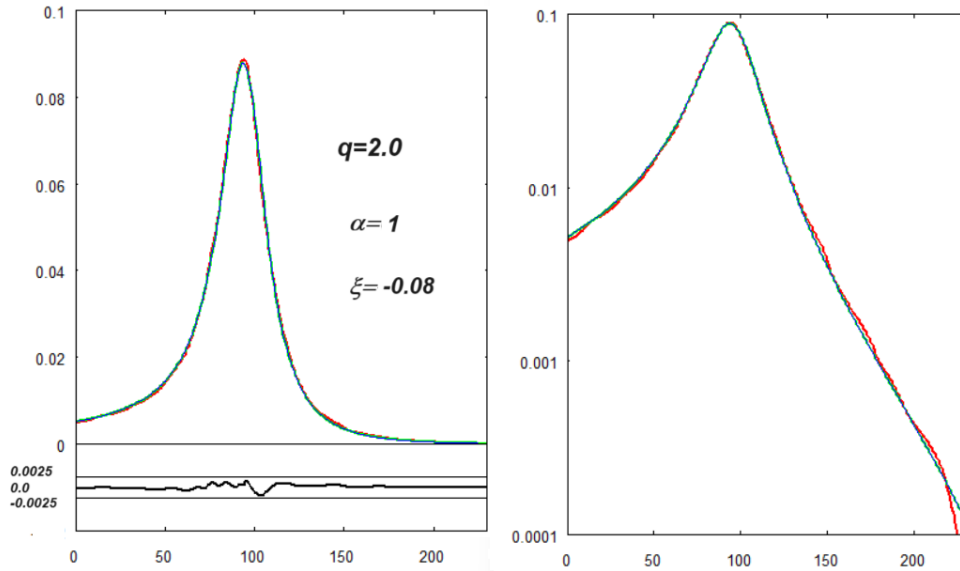
Fig. 1: The best fit (blue) onto the curve (red) given by Hasdeo et al. A q-BWF is used (the values of α, ξ and q-parameters are given in the figure. The misfit is proposed in the lower part of the plot. On the right, the same fit is shown with the log scale for y-axis (semi log scale). Data and q-BWF are given as functions of integers n (equally spaced points), for the x-axis which is representing the Raman shift. A convenient scale is used for the y-axis (intensity axis). The fitting calculation is obtained by minimizing the sum of the squares of the deviations (sum from n=1 to n=660). The value of this sum is 5.5 x 10^{-5}.

Let us consider the work by Campbell and Fauchet, 1986, and their Fig.4, with the peak for thin film of silicon on saphire (SOS).
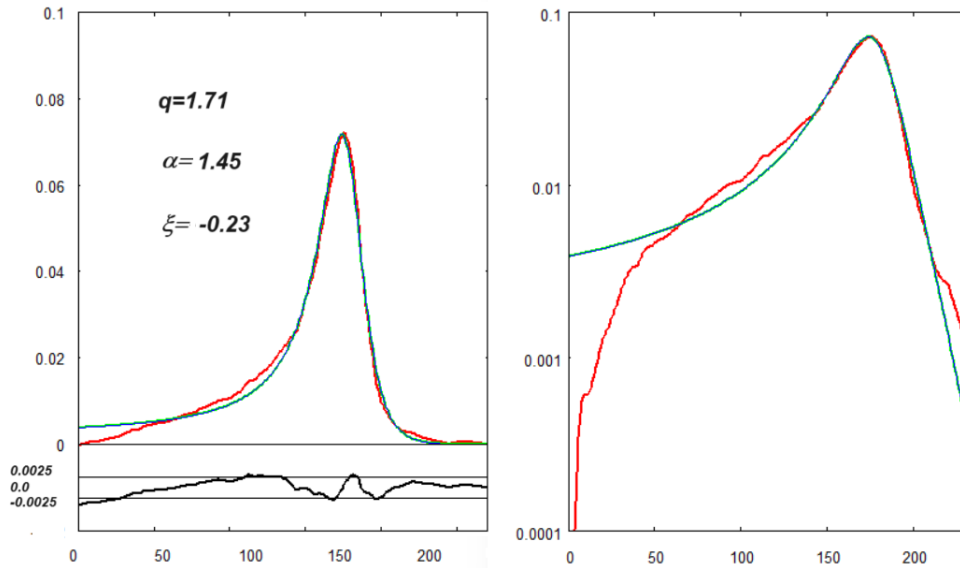

Fig. 2: The best fit (blue) onto the curve (red) given by Campbell and Fauchet, 1986. A q-BWF is used (the values ofα, ξ and q-parameters are given in the figure. The misfit is proposed in the lower part of the plot. The fitting calculation is obtained by minimizing the sum of the squares of the deviations (sum from n=1 to n=230). The value of this sum is 8.5 x 10^{-4}.

Then, let us apply the q-BWF to a specific case, that of the LO mode Raman band of SiC. Data are obtained from the Raman Open Database, a database which developed in the framework of project SOLSA H2020 (El Mendili et al., 2019), https://solsa.crystallography.net/rod/1000172.html .
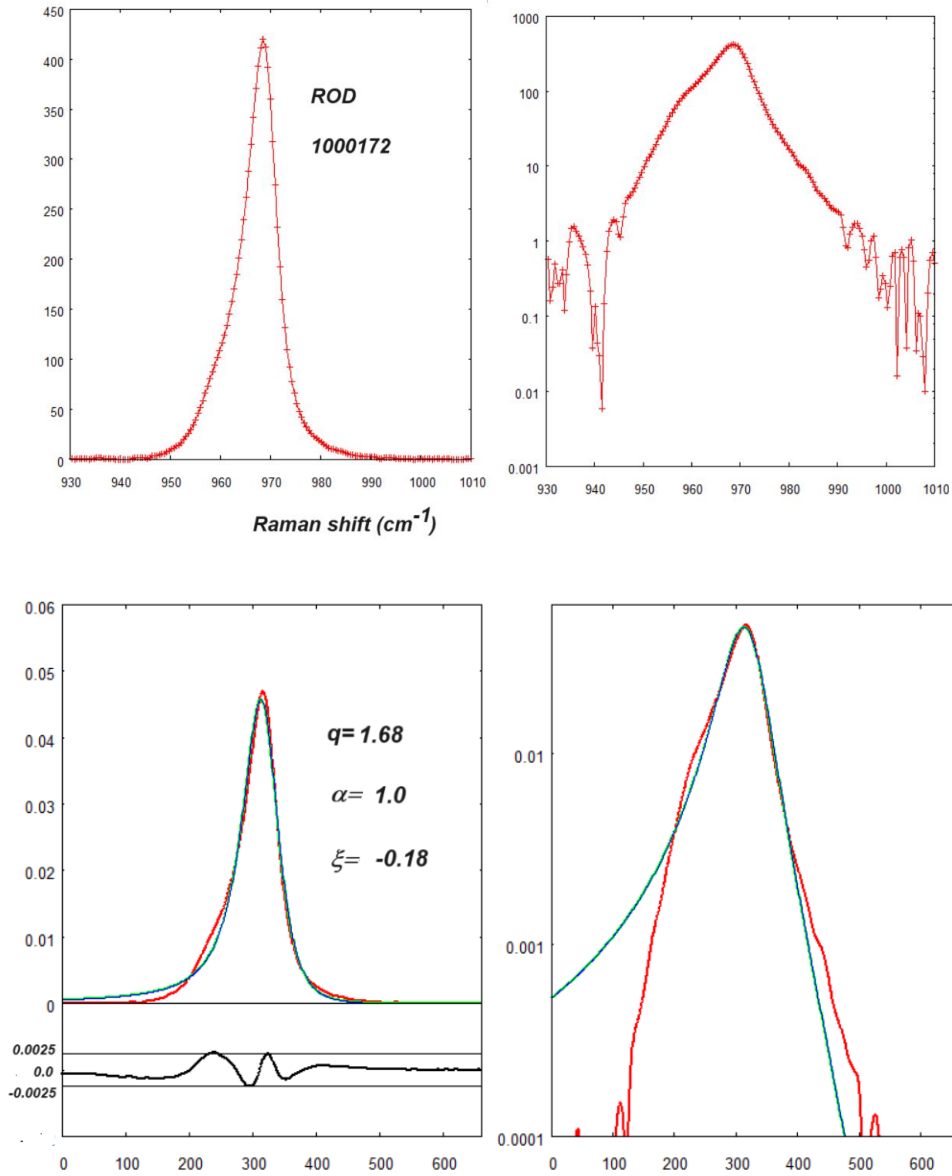
1

Fig.3: The best fit (blue) onto data (red) of ROD 1000172 (related ref. Capitani et al., 2007). On the right, the data with log scale y-axis (semi log scale). A q-BWF is used (the values of parameters are given in the figure. The fitting calculation is obtained by minimizing the sum of the squares of the deviations (sum from n=1 to n=660). The value of this sum is 6 .6 x 10^{-4}.

Remarks - Tsallis Gaussians can be easily compared with Gaussian and Lorentzian functions, and with pseudo-Voigtian functions too. In the same manner, the q-BWF can be easily compared to BWF function. Here we have proposed just three examples, but further studies are necessary to test the q-BWF.

References

1. Campbell, I. H., & Fauchet, P. M. (1986). The effects of microcrystal size and shape on the one phonon Raman spectra of crystalline semiconductors. Solid State Communications, 58(10), 739-741.
2. Capitani, G. C., Di Pierro, S., & Tempesta, G. (2007). The 6H-SiC structure model: Further refinement from SCXRD data from a terrestrial moissanite. American Mineralogist, 92(2-3), 403-407.
3. El Mendili, Y., Vaitkus, A., Merkys, A., Gražulis, S., Chateigner, D., Mathevet, F., Gascoin, S., Petit, S., Bardeau, J.-F., Zanatta, M., Secchi, M., Mariotto, G., Kumar, A., Cassetta, M., Lutterotti, L., Borovin, E., Orberger, B., Simon, P., Hehlen, B., & Le Guen, M. (2019). Raman Open Database: first interconnected Raman–X-ray diffraction open-access resource for material identification. Journal of Applied Crystallography, 52(3), 618-625. doi: 10.1107/s1600576719004229
4. Hanel, R., Thurner, S., & Tsallis, C. (2009). Limit distributions of scale-invariant probabilistic models of correlated random variables with the q-Gaussian as an explicit example. The European Physical Journal B, 72(2), 263.
5. Hasdeo, E. H., Nugraha, A. R., Dresselhaus, M. S., & Saito, R. (2014). Breit-Wigner-Fano line shapes in Raman spectra of graphene. Physical Review B, 90(24), 245140.
6. Kirillov, S. A. (2004a). Novel approaches in spectroscopy of interparticle interactions. Raman line profiles and dynamics in liquids and glasses. Journal of molecular liquids, 110(1-3), 99-103.
7. Kirillov, S. (2004b). Novel approaches in spectroscopy of interparticle interactions. Vibrational line profiles and anomalous non-coincidence effects. In Novel Approaches to the Structure and Dynamics of Liquids: Experiments, Theories and Simulations; Springer: Berlin/Heidelberg, Germany, 2004; pp. 193–227
8. Meier, R. J. (2005). On art and science in curve-fitting vibrational spectra. Vibrational spectroscopy, 2(39), 266-269.
9. Naudts, J. (2009). The q-exponential family in statistical physics. Central European Journal of Physics, 7, 405-413.
10. Prawer, S., & Nemanich, R. J. (2004). Raman spectroscopy of diamond and doped diamond. Philosophical Transactions of the Royal Society of London. Series A: Mathematical, Physical and Engineering Sciences, 362(1824), 2537-2565.
11. Richter, H., Wang, Z. P., & Ley, L. (1981). The one phonon Raman spectrum in microcrystalline silicon. Solid State Communications, 39(5), 625-629.
12. Sparavigna, A. C. (2022). Entropies and Logarithms. Zenodo. DOI 10.5281/zenodo.7007520
13. Sparavigna, A. C. (2023). q-Gaussian Tsallis Line Shapes and Raman Spectral Bands. International Journal of Sciences, 12(03), 27-40. http://dx.doi.org/10.18483/ijSci.2671
14. Sparavigna, A. C. (2023). q-Gaussian Tsallis Functions and Egelstaff-Schofield Spectral Line Shapes. International Journal of Sciences, 12(03), 47-50. http://dx.doi.org/10.18483/ijSci.2673
15. Sparavigna, A. C. (2023). q-Gaussian Tsallis Line Shapes for Raman Spectroscopy (June 7, 2023). SSRN Electronic Journal. http://dx.doi.org/10.2139/ssrn.4445044

16. Sparavigna, A. C. (2023). Formamide Raman Spectrum and q-Gaussian Tsallis Lines (June 12, 2023). SSRN Electronic Journal. http://dx.doi.org/10.2139/ssrn.4451881

17. Sparavigna, A. C. (2023). Tsallis and Kaniadakis Gaussian functions, applied to the analysis of Diamond Raman spectrum, and compared with Pseudo-Voigt functions. Zenodo. https://doi.org/10.5281/zenodo.8087464

18. Sparavigna A. C. (2023). Tsallis q-Gaussian function as fitting lineshape for Graphite Raman bands. ChemRxiv. Cambridge: Cambridge Open Engage; 2023.

19. Sparavigna A. C. (2003). Fitting q-Gaussians onto Anatase TiO2 Raman Bands. ChemRxiv. Cambridge: Cambridge Open Engage; 2023.

20. Sparavigna, A. (2023). Q-Gaussians and the SERS Spectral Bands of L-Cysteine and Cysteamine. ChemRxiv. doi:10.26434/chemrxiv-2023-9swp9-v2

21. Tsallis, C. (1988). Possible generalization of Boltzmann-Gibbs statistics. Journal of statistical physics, 52, 479-487.

22. Tsallis, C. (1995). Some comments on Boltzmann-Gibbs statistical mechanics. Chaos, Solitons & Fractals, 6, 539-559.

23. Umarov, S., Tsallis, C., Steinberg, S. (2008). On a q-Central Limit Theorem Consistent with Nonextensive Statistical Mechanics. Milan J. Math. Birkhauser Verlag. 76: 307–328. doi:10.1007/s00032-008-0087-y. S2CID 55967725.